Dalton Transactions

Accepted Manuscript

Volume 45 | Number 1 | 7 January 2016 | Pages 1–398

Dalton Transactions

An international journal of inorganic chemistry
www.rsc.org/dalton

ISSN 1477-9226

ROYAL SOCIETY OF CHEMISTRY

PAPER
Joseph T. Hupp, Omar K. Farha et al.
Efficient extraction of sulfate from water using a Zr-metal–organic framework

175 YEARS

ROYAL SOCIETY OF CHEMISTRY

rsc.li/dalton

Journal Name

COMMUNICATION

Fe(III)-doped coordination polymer of Mn₁₃-clusters with improved activity for oxygen reduction reaction

Tian Wen[a], Wolfgang Schmitt[b] and Lei Zhang[a]*

Fe(III) dopants have been introduced to a porous coordination polymer of Mn₁₃-clusters to form composite materials. The resulting Fe@Mn₁₃-polymer showed enhanced oxygen reduction reaction (ORR) activity, making it a low-cost and noble-metal-free ORR electrocatalyst.

The search for clean and renewable energy sources has attracted tremendous attention due of the ever-increasing consumption of fossil fuels and worldwide environmental crisis.[1-5] New sustainable energy concepts rely on the fabrication of high-efficiency electrochemical energy storage and conversion devices and the development of oxygen reduction reaction (ORR) catalysts.[6-11] To date, Pt-based ORR catalysts have been extensively explored and reveal the highest activity.[12-13] However, the scarcity and high-cost of Pt materials have greatly limited their large-scale applications. Thus, it becomes desirable to develop alternative ORR catalysts of cheap and abundant transition metals. Among them, Fe is one of the most promising candidates and many Fe-based ORR catalysts have been reported.[14-18] Although many progresses have been achieved, it still remains a challenge to improve the electrochemical activity and stability of Fe-based ORR catalysts.

The capacity and atomic utilization efficiency of catalysts are greatly influenced by their morphology and size. Accordingly, ultra-small nanoparticles or even single-atom Fe-catalysts have recently been investigated, achieving enhanced ORR activities.[19] However, such atomic catalysts suffer from their strong tendency towards aggregation. To solve this problem, porous matrixes have been applied to support and stabilize the single-atom Fe-catalysts, including metal-organic frameworks (MOFs) and porous carbon frameworks.[20-21] From the view of structural design, such porous materials can also provide a tool to further tune the activity of the designed complex catalysts

beyond the role of support. Especially, additional functionality could be incorporated if the nodes of the porous matrixes were transition metal clusters, which themselves impart ORR activity.

Scheme 1 Illustration for the construction of Fe@Mn₁₃-polymer composites.
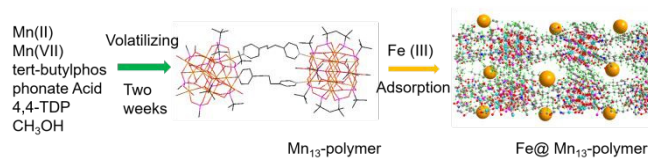
Considering other earth-abundant catalysts, manganese oxide has also been confirmed to be a promising, non-noble metal ORR catalyst with high performance.[22] Similarly, molecular oxide analogues, Mn-oxo clusters, should also have potential to reduce oxygen. Thus, the combination of Fe catalysts and Mn clusters within one ORR system might give rise promising synergistic advantages. Following this consideration, we applied a porous coordination polymer of Mn₁₃-oxo clusters to distribute and stabilize individual Fe(III) irons at molecular level and evaluate the ORR performance. Thus, the catalytic system distinguishes itself from bulk clusters or nanoparticles to form complex catalyst.

In our previous work, we employed a 1D Mn₁₃-polymer with distinctive pore diameters (*ca.* 10 × 12 Å) to adsorb TCQN molecules and encapsulate CdS nanoparticles to enhance the photocatalytic H₂ production.[23-24] Herein, taking advantage of the supramolecular channels of the Mn₁₃-polymer, we further introduced Fe(III) dopants into the Mn₁₃-oxo cluster-based framework *via* a two-step fabrication method to form Fe@Mn₁₃-polymer composites (Scheme 1). The obtained materials were characterized by several analytical methods including transmission electron microscopy (TEM), energy dispersive X-ray (EDX) spectra and the elemental mapping, and X-ray photoemission spectroscopy (XPS). Moreover, the obtained Fe@Mn₁₃-polymer displayed enhanced catalytic ORR activity in 0.1 M KOH solution.

[a.] School of Chemistry, The University of Melbourne, Parkville, Victoria 3010, Australia. E-mail: lei.zhang1@unimelb.edu.au
[b.] School of Chemistry & CRANN, University of Dublin, Trinity College, Dublin 2, Ireland.

COMMUNICATION

Microcrystals of the Mn_{13}-polymer were synthesized *via* a reported solvothermal method.[23] The freshly prepared Mn_{13}-samples were then immersed into an aqueous solution of $FeCl_3$ for 24 hours as described in the experimental section (see ESI for details). Prior to the electrocatalytic studies of the composite material, the structural attributes and stability of the prepared $Fe@Mn_{13}$-polymer was investigated. The powder X-ray diffraction (PXRD) analysis confirmed that the porous framework of the original Mn_{13}-polymer remained unchanged upon Fe^{3+} uptake (Figure S1). Fourier transform infrared spectroscopy (FT-IR) was used to undoubtedly identify the presence of the organic ligands. The IR bands at ~982, 1100 and 2919 cm^{-1} (Figure S2), originate from the bending vibrations of C–N, C–C moieties and from C–H stretching vibrations, respectively. Raman spectra also confirmed the presence of terminal *tert*-butylphosphonate ligands which resulted in signals at 960-990 cm^{-1} (Figure S3). Furthermore, the solid-state UV-vis spectrum of original Mn_{13}-polymer exhibited two characteristic bands at 245 and 451 nm (Figure S4). However, the UV–vis spectrum of $Fe@Mn_{13}$-polymer showed a broad band between 200-600 nm, which might be attributed to charge transfer interactions between the Mn_{13}-polymer and Fe(III) dopants.

The morphology of the obtained $Fe@Mn_{13}$-polymer was characterized by scanning electron microscopy (SEM) and transmission electron microscopy (TEM). As shown in Figure 1a, after immobilization, the samples of $Fe@Mn_{13}$-polymer retain their well-defined crystalline morphology. The obtained TEM images were that of a homogeneous sample, indicating that there was no aggregation of bulk metal or oxide nanoparticles (Figure 1b). In addition, no lattice fringes of crystallized Fe or Mn oxides were detected by the high-resolution TEM (Figure 1c), further suggesting that the structure of the Mn_{13}-polymer was stable and no bulk metal oxides particles were formed during the Fe(III) ion absorption process. Moreover, results of energy dispersive X-ray (EDX) spectroscopy and the element mapping confirmed the homogeneous distribution of Fe dopants in the prepared $Fe@Mn_{13}$-polymer material (Figures 1d-f, S1). Furthermore, the Fe(III) uptake was calculated to be *ca.* 0.45 wt% as determined by inductively coupled plasma-mass (ICP) spectrometry analysis.
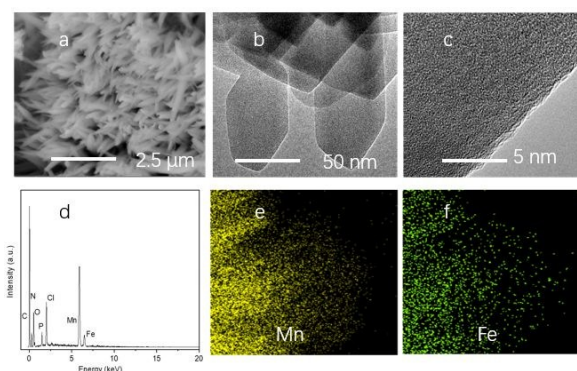

Figure 1. Morphology and composition analysis of the $Fe@Mn_{13}$-polymer sample: (a) SEM, (b) TEM and (c) HRTEM images. (d) EDX spectrum and (e, f) elemental mapping.

To further analyze the composition and chemical states of the prepared $Fe@Mn_{13}$-polymer material, high resolution XPS studies were performed. The obtained spectra confirmed the presence of Fe, Mn, C, O, P, N and Cl elements (Figure 2a). As shown in Figure 2b, the XPS spectrum in the Mn 2p region presented two strong peaks at 652.9 and 642.3 eV, which can be assigned to Mn 2p1/2 and 2p3/2, respectively. The Fe 2p region showed two main peaks at 712.8 and 725.6 eV of Fe 2p3/2 and Fe 2p1/2 (Figure 2c), suggesting that the oxidation state of the Fe dopants in the $Fe@Mn_{13}$-polymer is +III. The O 1s spectrum can be divided into two peaks (Figure 2d), whereby one signal at 531.7 eV derives from P=O moieties and the one at 533.2 eV can be attributed to OH groups.
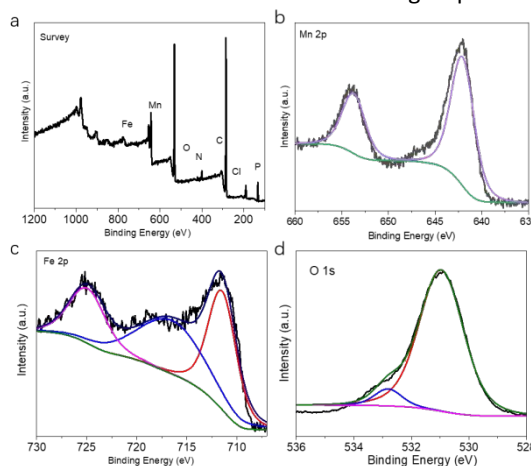

Figure 2. (a) XPS survey spectrum of the $Fe@Mn_{13}$-polymer. High resolution XPS spectrum of Fe@Mn13-polymer in the (b) Mn 2p, (c) Fe 2p and (d) O 1s regions.

The above results demonstrated that the structure of the Mn_{13}-polymer remained almost unchanged after Fe(III) dopants were successfully introduced. Then the ORR activity of the prepared $Fe@Mn_{13}$-polymer was tested in an O_2 saturated 0.1m KOH solution using a rotating disk electrode set-up (Figure 3). The linear sweep voltammetry (LSV) results indicated that the $Fe@Mn_{13}$-polymer showed the best activity in terms of the most positive onset potential. As shown in Figure 3b, the E1/2 of the $Fe@Mn_{13}$-polymer was 0.70 V, which was 50 mV more positive than that of the pure Mn_{13}-polymer, highlighting the important role of Fe(III) dopants to improve the ORR activity. Also, the Tafel slope value of the $Fe@Mn_{13}$-polymer is 130 mV dec^{-1}, which is significantly smaller than 265 mV dec^{-1} of the pure Mn_{13}-polymer (Figure S7), indicating better ORR activity. The electrochemical impedance spectroscopy (EIS) was also investigated to gain insights into charge transport processes that relate to the catalyst conductivity. The semicircular diameter in the EIS of the $Fe@Mn_{13}$-polymer is smaller than that of the unmodified Mn_{13}-polymer (Figure S8). On the one hand, the smaller charge transfer impedance implies better access of the O_2 containing electrolyte to the $Fe@Mn_{13}$-polymer surface and faster charge transfer on the surface and within the structure, in comparison to the native Mn_{13}-polymer, which is a direct result of the Fe-doping within the porous structure of Mn_{13}-polymer. On the other hand, the smaller semicircular diameter in the EIS of the $Fe@Mn_{13}$-polymer contributes to shuttle charges from the catalyst to the O_2 substrate, which increased ORR affection with a higher diffusion limiting current density. Thus, the synergistic effect of Fe dopants and Mn_{13}-polymer

Dalton Transactions Accepted Manuscript

Journal Name

COMMUNICATION

resulted in improved ORR activity. Although the activity of the hybrid Fe@Mn$_{13}$-polymer is lower than Pt/C (Figure S6), it is still of significance as a noble-metal-free ORR electrocatalyst.
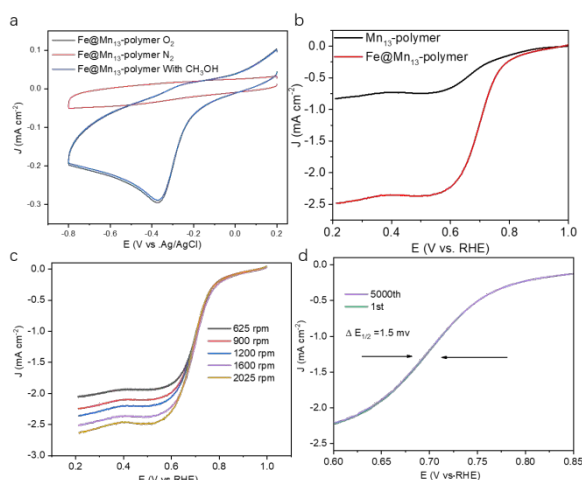

Figure 3. (a) Cyclic voltammograms (CV) of Fe@Mn$_{13}$-polymer electrocatalysts in 1.0M CH$_3$OH, N$_2$- and O$_2$-saturated 0.1M solution of KOH with a scan rate of 0.1 V/s. (b) LSV of various electrocatalysts in an O$_2$-saturated 0.1 M aq KOH solution (scan rate: 10 mVs^{-1}). (c) ORR polarization curves of Fe@Mn$_{13}$-polymer at different rotating rates. (d) ORR polarization curves before after 5000 potential cycles.

To examine the fuel crossover effect, Fe@Mn$_{13}$-polymer samples were cycled in both O$_2$-stratured 0.1 M KOH and O$_2$-stratured 0.1 M KOH + 1.0 M methanol solutions. There were no obvious changes of the current density in the presence of the Fe@Mn$_{13}$-polymer after injecting methanol into the solution (Figure 3a), demonstrating that the Fe@Mn$_{13}$-polymer had excellent tolerance to methanol crossover. The applied Mn$_{13}$-polymer contains rich tert-butylphosphonate ligands with hydrophobic-CH$_3$ group, endowing it with high aqueous stability. The Fe and Mn atoms in the hybrid Fe@Mn$_{13}$-polymer are both alterable valent ions, possibly contributing to the electrochemical flexibility and stability. The stability and durability of the Fe@Mn$_{13}$-polymer were then assessed by cycling tests between 0.6 and 1.0 V at a sweep rate of 50 mV s^{-1} in O$_2$-saturated 0.1 M KOH. After 5000 continuous cycles (Figure 3 d), only minor changes in E1/2 (*ca.* ~1.5 mV) were observed. Moreover, after the CV tests, the LSV and IR spectra of Fe@Mn$_{13}$-polymer were almost unchanged (Figure S1, S9).

In conclusion, for the first time, coordination polymers based on Mn-clusters have been applied as noble-metal-free ORR electrocatalysts. Taking the advantage of its porous structure, Fe(III) doped Mn$_{13}$-polymer composite catalysts were synthesized and characterized. Electrochemical studies confirmed that the obtained Fe@Mn$_{13}$-polymer revealed enhanced and stable ORR activity. Therefore, this work highlights the potential of Mn coordination clusters as low-cost ORR electrocatalysts and may open an avenue to cheaper and environmentally-friendly electrolysis.

Conflicts of interest

There are no conflicts of interest to declare.

References

1 N. S. Lewis and D. G. Nocera, *Proc. Natl. Acad. Sci. U. S. A.*, 2006, **103**, 15729–15735.

2 J. Lin, Y. Dong, Q. Zhang, D. Hu, N. Li, L. Wang, Y. Liu and T. Wu, *Angew. Chem., Int. Ed.*, 2015, **54**, 5103–5107.

3 J. Suntivich, H. A. Gasteiger, N. Yabuuchi, H. Nakanishi, J. B.Goodenough and Y. Shao-Horn, *Nat. Chem.*, 2011, **3**, 546–550.

4 P. G. Bruce, S. A. Freunberger, L. J. Hardwick and J.-M. Tarascon, *Nat. Mater.*, 2011, **11**, 19–29.

5 Debe, M. K. *Nature* 2012, **486**, 43–51.

6 L. Chih-Ping, G. Wang, A. Kumar and V. Ramani, *Appl.Catal., B, 2013*, **140**, 133–140.

7 H. Peng, F. Liu, X. Liu, S. Liao, C. You, X. Tian, H. Nan,F. Luo, H. Song, Z. Fu and P. Huang, *ACS Catal.*, 2014, **4**, 3797–3805.

8 B. P. Vinayan, T. Diemant, R. J. Behm and S. Ramaprabhu, *RSC Adv.*, 2015, **5**, 66494–66501.

9 A. Muthukrishnan, Y. Nabae, T. Hayakawa, T. Okajima and T. Ohsaka, *Catal. Sci. Technol.*, 2015, **5**, 475–483.

10 J. Wang, G. Wang, S. Miao, J. Li and X. Bao, *Faraday Discuss.*, 2014, **176**, 135–151.

11 G. Wang, W.-H. Wang, Li.-K. Wang, W.-T. Yao, P.-F. Yao,W.-K. Zhu, P. Chen and Q.-S. Wu, *J. Mater. Chem. A*, 2015, **3**, 17866–17873.

12 K. K. Tintula, A. K. Sahu, A. Shahid, S. Pitchumani,P. Sridhar and A. K. Shukla, *J. Electrochem. Soc.*, 2011, **158**, B622–B631.

13 A. Arunchander, S. G. Peera, V. Parthiban, S. Akula, K. K. Tintula, S. D. Bhat and A. Kumar Sahu, *RSC Adv.*, 2015, **5**, 75218–75228.

14 S.-H. Liu, J.-R. Wu, C.-J. Pan and B.-J. Hwang, *J. Power Sources*, 2014, **250**, 279–285.

15 W. J. Jiang, L. Gu, L. Li, Y. Zhang, X. Zhang, L. J. Zhang, J. Q. Wang, J. S. Hu, Z. Wei, L. J. Wan, *J. Am. Chem. Soc.* 2016, **138**, 3570–3578

16 J. Wang, Z. Q. Huang, W. Liu, C. R. Chang, H. L. Tang, Z. J. Li, W. X. Chen, C. J. Jia, T. Yao, S. Q. Wei, Y. Wu, and Y. D. Li, *J. Am. Chem. Soc.* 2017, **139**, 17281−17284.

17 Y. J. Sa, D.J. Seo, J. Woo, J.T. Lim, J. Y. Cheon, S. Y. Yang, J. M. Lee,D. Kang, T. J. Shin,H. S. Shin, H. Y. Jeong, C. S. Kim, M. G. Kim, T. Y. Kim and S. H. Joo, *J. Am. Chem. Soc.* 2016, **138**, 15046 −15056

18 G. Yang, W. Choi, X. Pu and C. Yu *Energy Environ. Sci.,* 2015, **8**, 1799−1807

19 J.-C. Li, Z.-Q. Yang, D.-M. Tang, L.-L. Zhang, P.-X. Hou, S.-Y. Zhao,C. Liu, M. Cheng, G.-X. Li, F. Zhang and H.-M. Cheng, *NPG Asia Materials* 2018,**10**, e461.

20 Y. J. Chen, S. F. Ji, Y. G. Wang, J. C. Dong, W. X. Chen, Z. Li, R. G. Shen, L. R. Zheng, Z. B. Zhuang, D. S. Wang and Y. D. Li, *Angew. Chem. Int. Ed.* 2017, **56**, 6937–6941.

21 J. Zhang, D. He, H. Su, X. Chen, M. Pan and S. Mu, *J. Mater. Chem. A*, 2014, **2**, 1242–1246.

22 K. A. Stoerzinger, M. Risch, B. Han and Y. Shao-Horn, *ACS Catal.*, 2015, **5**, 6021–6031.
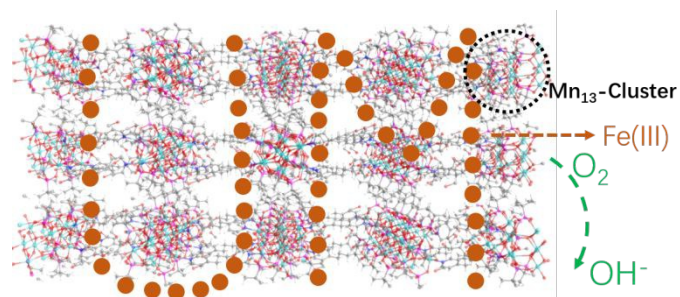
COMMUNICATION

23 L. Zhang, R. Clérac, C. I. Onet, M. Venkatesan, P. Heijboer and W. Schmitt, *Chem. – Eur. J.*, 2012, **18**, 13984–13988.

24 T. Wen, L. Zhang and W. Schmitt, *Dalton Trans.,* 2018, **47**, 10857–10860.

COMMUNICATION

Homogeneously distributed Fe(III) dopants were introduced into porous coordination polymers of Mn$_{13}$-clusters to form composite materials. The resulting Fe@Mn$_{13}$-polymer exhibited efficient oxygen reduction reaction (ORR) activity.

Dalton Transactions Accepted Manuscript